

geophysical prospecting 42, 179-276

geophysical prospecting

A study of the geoelectrical properties of peatlands and their influence on ground-penetrating radar surveying. <i>Brian D. Thelmer, David C. Nobes and Barry G. Warner</i>	179
Layer-stripping reverse-time migration. <i>Ruey-Chyuan Shih and Alan R. Leander</i>	211
Relation of <i>in situ</i> resistivity to water content in salt rocks. <i>U. Yerramanuri</i>	229
Ground events decomposition and the interaction between AVO and velocity information. <i>Umberto Spagnolini</i>	241
A method to estimate the total magnetization direction from a distortion analysis of magnetic anomalies. <i>Maurizio Fedi, Giovanni Florio and Antonio Rapolla</i>	261
Errata	275



European Association of Exploration Geophysicists

1994 Publication Schedule

- Volume 42:1 January
- Volume 42:2 February
- Volume 42:3 April
- Volume 42:4 May
- Volume 42:5 July
- Volume 42:6 August
- Volume 42:7 October
- Volume 42:8 November

BLACKWELL SCIENTIFIC PUBLICATIONS
 Osney Mead, Oxford OX2 0EL
 25 John Street, London WC1N 2BL
 23 Ainslie Place, Edinburgh EH3 6AJ
 Suite 500, 5th Floor, 238 Main Street, Cambridge,
 MA 02142, U.S.A.
 54 University Street, Carlton, Victoria 3053, Australia

Other BSP Editorial Offices:
 Arnette SA, 1 Rue de Lille, 75006 Paris, France
 Blackwell Wissenschaft-Verlag GmbH, Düsseldorf Strasse 38,
 D-10707 Berlin, Germany
 Blackwell MZV, Feldgasse 13, A-1238 Vienna, Austria



April 1994

GPPRAR42 (3) 179-276 (1994)
 ISSN 0016-8025
 Volume 42 Number 3
 April 1994

Compound events decomposition and the interaction between AVO and velocity information¹

Umberto Spagnolini²

Abstract

Minimization of seismic residuals does not guarantee uniqueness of the model, and this implies ambiguities in the inversion. Amplitude vs. offset (AVO) inversion does not lead to a unique solution of single elastic interface parameters unless converted and S-wave or critical angle reflections are available. Given the ambiguity of AVO inversion, this paper discusses the interaction between AVO and velocity estimation. The number of independent parameters necessary to describe an isolated reflection with AVO behaviour and residual velocity error is determined. Statistical analysis allows the establishment of an approximate equivalence of the effects of AVO and slight velocity variations; this equivalence cannot be solved without geological *a priori* information (kinematic equivalence). The data are then decomposed into compound events (i.e. sequences of N interfaces that follow each other at a fixed time lag). The decomposition is obtained by extrapolating the results of the analysis from narrowband to wideband data. Compound events decomposition demonstrates that AVO inversion is ambiguous, not only in the physical parameter space (P- and S-wave velocities, and density) but also kinematically. As an example of compound event decomposition, a medium is derived. This medium is geologically implausible but is kinematically equivalent.

Introduction

Accurate velocity estimation is essential to the post-stack and prestack processing (e.g. depth migration) of seismic data. Prestack analysis allows, in principle, the estimation of elastic parameters (P- and S-wave velocities, density). The usual approach considers a sequence of unknown elastic interfaces that are estimated using a suitable minimization of the data residuals. Further constraints can improve the quality of the results in a full elastic inversion (Tarantola 1986, 1987; Kolb, Collino and Lailly 1986). However, it is still necessary to understand fully the limits and reliability of the inversion technique. The minimization of the

¹ Received February 1993, revision accepted November 1993.

² Dipartimento di Elettronica e Informazione, Politecnico di Milano, Piazza L. da Vinci, 32, I-20133 Milano, Italy.

residuals is not enough to guarantee that the proposed model is the real one (ambiguity of the inversion).

Amplitude and phase vs. offset (AVO and PVO) measurement is an alternative approach to elastic parameter estimation. In AVO and PVO the elastic model is simplified as a disjoint sequence of interfaces. The sparse interfaces assumption is necessary for reliable AVO and PVO measurements. AVO inversion searches for those optimal elastic parameters that fit the AVO measurements. Noise-free AVO inversion is also ambiguous. The need to use not only P-P reflections but also P-S, S-S and S-P reflections to improve the reliability of the interface inversion was discussed by de Haas and Berkhout (1990) and Van Rijssen and Herman (1991). Moreover the reliability of the inversion is reduced by AVO measurement errors. Single-interface AVO measurement requires:

1. a more accurate kinematic model than that allowed by seismic imaging;
2. a 'true' amplitude preserving processing;
3. a reliable AVO analysis technique.

In addition, Folstad and Schoenberg (1992) have demonstrated that an equivalent elastic medium obtained as a layered model of transversely anisotropic elastic layers has a wavefield comparable to the measured one, provided that the layer thickness is of the order of 1/10 of the smallest wavelength (the equivalence is approximately within 2-3% of the residual).

A key role in AVO analysis for elastic parameter estimation is played by velocity analysis; even small errors can cause quite relevant inaccuracies in the estimation of the proper AVO. It was shown by Spratt (1987) and Walden (1991) that velocity error, or residual normal moveout (RNMO), reduces the reliability of AVO measurements. NMO correction and stretching reduces the accuracy of AVO measurements (Herbert 1991) so it is advisable, when AVO measurements are employed, to correct moveout statically. In AVO analysis the bandwidth of the wavelet must be considered when estimating the reflection moveout. It must be stressed again that if AVO analysis is performed to look for isolated reflections, signal muting should be used to reduce reflection interference.

The sparse interfaces assumption is partially removed in this study and the velocity error is considered. Each reflection, or combination of interfering reflections with AVO and velocity errors, is decomposed into a fixed basis of compound events: compound events decomposition (CED). A compound event of the N th order is a sequence of N interfaces that follow each other at a fixed time lag, usually much longer than the sampling interval and pre-assigned RNMO. The events belonging to the compound event may or may not exhibit AVO behaviour. First, a statistical analysis of the interaction between AVO and RNMO is presented. Any narrowband elastic reflection (assumed here to have a physically plausible AVO behaviour), unknown deterministically but characterized by a known statistical distribution of the AVO and RNMO parameters, is projected onto the basis of a compound event with or without AVO. For instance, classical AVO analysis, plus a small velocity error, corresponds to a compound event with $N = 1$.

By increasing the order N , the CED spans the data space more accurately. The compound event corresponds to an equivalent medium, perhaps geologically implausible.

Elastic reflections model

Consider the common midpoint (CMP) gather of a horizontally layered earth. The model of P-P reflections is simplified to obtain a simple expression of the interaction between AVO and velocity errors.

• The reflection times can be represented by the series $t^2(x) = \tau^2 + (1/v^2)x^2 + c_2 x^4 + c_3 x^6 + \dots$, where τ is the normal incidence traveltime and v is the velocity. Only short offsets or small angles of incidence are considered in this simplified model so that the following parabolic moveout approximation holds true:

$$t(x) \simeq \tau + \frac{x^2}{2\tau v^2} = \tau + px^2, \quad (1)$$

where p is the moveout parameter. However, considering residual moveout, the parabolic approximation holds even for larger offsets.

• The amplitude of the reflections vs. offset x (AVO) is approximated by the relation $A + Bx^2 = A(1 + qx^2)$, where q is the AVO parameter normalized to zero-offset amplitude A . Assuming that only small angles of incidence are considered ($\theta < 30^\circ$), Shuey (1985) showed that the P-P reflection coefficient ($R_{pp}(\theta)$) depends approximately on both P-P ($R_{pp}(0)$) and S-S ($R_{ss}(0)$) normal incidence reflectivity, i.e.

$$R_{pp}(\theta) \simeq R_{pp}(0) + [R_{pp}(0) - 2R_{ss}(0)] \sin^2 \theta. \quad (2)$$

Assuming a layered medium, the relationship between $\sin^2 \theta$ and the offset can be easily derived (e.g. Walden 1991). The zero-offset amplitude A depends on the acoustic impedance contrast, whereas the S-S normal incidence reflectivity can be estimated from the AVO parameter q .

• The seismic wavelet $w(t)$ considered here has no phase shift vs. offset (PVO). The reflection model chosen deals first with narrowband and then with limited and wideband wavelets. Narrowband analysis that considers phase shifts instead of time delays allows a general statistical analysis of the equivalence between AVO and RNMO. Wideband analysis is complicated by the additional degree of freedom of the time delay.

Avoiding, in this section, a detailed discussion of the processing steps (e.g. multiples removal, geometrical spreading correction and transmissivity correction of the upper layers), the CMP seismic signal $s(x, t)$ can then be simplified as a linear combination of simple events with their AVOs, given by

$$s(x, t) = \sum_i A_i (1 + q_i x^2) w(t - \tau_i - p_i x^2). \quad (3)$$

The residual between the data $d(x, t)$ and the signal given by $\iint |d(x, t) - s(x, t)|^2 dt dx$, is used in the estimation of the following parameters of the i th event:

τ_i, p_i : kinematic parameters that mainly influence the P-wave velocity V_p and layer thickness (macro velocity model);

A_i, q_i : AVO parameters that can be used for the estimation of the elastic parameters of the interface (a more detailed kinematic model, density ρ and S-wave velocity V_s).

The minimization of the residual is quadratic in the AVO parameters and non-linear in the kinematic parameters. Since the distinction between the macromodel parameters obtained from the kinematics and the detailed description of the interface from the AVO analysis cannot be exact, in the next section the interaction between AVO and RNMO of seismic data will be analysed qualitatively.

Interaction between AVO and kinematic parameters

AVO provides additional information with respect to the kinematic parameters for elastic interface evaluation. Given the seismic data, the velocity and AVO analysis can be seen as a way to decompose the data into amplitude parameters (projection onto the AVO subspace $\{A\}$) and kinematic parameters (projection onto the kinematic subspace $\{K\}$). Referring to the introduced formalism, (τ, p) belongs to the kinematic subspace $\{K\}$ while (A, q) belongs to the AVO subspace $\{A\}$. The interaction between AVO and RNMO can be represented as a non-orthogonality between AVO and kinematic subspaces used for data decomposition (Fig. 1). In other words, as $\{A\}$ and $\{K\}$ are not orthogonal, there is a crosstalk between AVO and RNMO; however, this corresponds to different media.

The interaction between RNMO and AVO of an NMO corrected elastic reflection in the (x^2, t) domain can be analysed in the Fourier transformed domain (k_{x2}, ω) . The spectrum of an isolated reflection with AVO could be considered as the super-position of two or more events, each at a constant value of the wavenum-

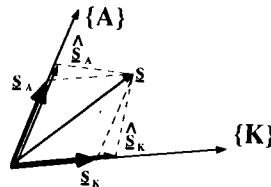


Figure 1. Representation of non-orthogonality between AVO subspace $\{A\}$ and kinematic subspace $\{K\}$. Given the seismic data $S = s(x, t)$, the true kinematic s_k and amplitude s_A parameters should be estimated. As $\{A\}$ and $\{K\}$ are non-orthogonal, there is a crosstalk between RNMO and AVO in the estimated \hat{s}_k and \hat{s}_A .

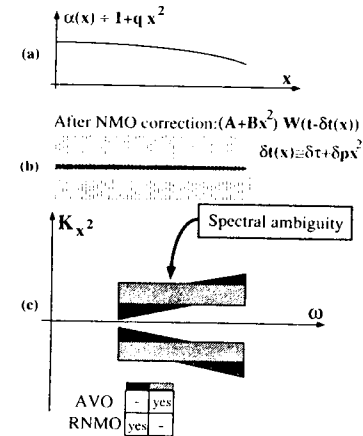


Figure 2. The interaction between AVO and RNMO in the spectral domain. Seismic data with a given AVO (a) and after NMO correction (b) can be analysed in the Fourier transformed domain (k_{x2}, ω) . (c) An equivalent reflection with AVO and without RNMO and two reflections without AVO but with velocity errors share the same spectrum (spectrum ambiguity). The interaction depends on the wavelet bandwidth and on the maximum offset.

ber k_{x2} as shown in Fig. 2. Considering two or more reflections with different RNMO, without any amplitude change vs. offset, their spectra are on separate slopes, each depending on the reflection RNMO parameter $p_i, i = 1, 2$ (Fig. 2). Time resolution is limited by wavelet bandwidth, whereas the maximum offset limits the RNMO resolution; this leads to ambiguity in the spectra. The spectrum of an isolated reflection with AVO can be interpreted as a superposition of two or more reflections without AVO.

Narrowband decomposition

Eigenvector decomposition

The elastic reflections of a quasi-sinusoidal medium (narrow bandwidth) are considered in order to analyse the interaction of AVO and RNMO; furthermore the number of degrees of freedom of the seismic signal generated with a random distribution of the AVO and RNMO parameters is evaluated.

After NMO correction, the elastic reflection is characterized by normalized RNMO (p), AVO (q), at frequency ω_0 ; sampling at points x_1, \dots, x_n along the offset, gives the data vector

$$a(p, q) = A[(1 + qx_1^2)e^{j\omega_0 p x_1^2}, \dots, (1 + qx_n^2)e^{j\omega_0 p x_n^2}], \quad (4)$$

([.] indicates matrix transposition). The offset is normalized to the maximum offset ($x_{\max} = 1$) and the maximum RNMO herein considered gives a phase difference of $|\omega_0 p x_{\max}^2| \leq \omega_0 x_{\max}^2 = \pi$ over the cable length so that the normalized RNMO parameter is now limited $|p| \leq 1$ (i.e. this value corresponds to a limit of the velocity errors equal to half the wavelength at the cable's end).

Each elastic reflection in the time window could be characterized by RNMO and AVO behaviour that is not deterministically known *a priori*; it can be modelled by its statistical distribution. In other words, let us suppose that the probability densities of AVO, $g(q)$, and RNMO, $f(p)$, are known. The covariance matrix for independent events (the normal-incidence reflection coefficients are taken as zero-mean statistically-independent variables) is

$$\mathbf{R} = \iint \mathbf{a}(p, q) \mathbf{a}^*(p, q) f(p) g(q) dp dq = E[\mathbf{a} \mathbf{a}^*], \quad (5)$$

where the notation * here indicates the conjugate transposition. The number of non-negligible eigenvalues of \mathbf{R} indicates the number of degrees of freedom of the data, i.e. the number of independent parameters that can be used to model the data. In fact the eigenvectors $\mathbf{v}_i, i = 1, \dots, N$ of the covariance matrix \mathbf{R} completely span the data subspace, provided that the eigenvalues are $\lambda_1 > \lambda_2 > \dots > \lambda_N > \lambda_{N+1} \approx \lambda_{N+2} \approx \dots \approx \lambda_n = 0$, ($\text{Rank}\{\mathbf{R}\} = N$). Each event considered in the modelled distribution of AVO and RNMO can be obtained as a linear combination of the N eigenvectors spanning the data subspace:

$$\mathbf{a}(p, q) = \sum_{i=1}^N \beta_i(p, q) \mathbf{v}_i + \boldsymbol{\varepsilon}(p, q), \quad (6)$$

so that the residual $\|\boldsymbol{\varepsilon}(p, q)\|^2 \approx 0$.

Considering a uniform (i.e. equally likely) distribution of AVO and RNMO between the two extreme values ($|q| \leq 1$ and $|p| \leq p_{\max} = 1$), the number of degrees of freedom is $N = 3$, as shown in Fig. 3 where the eigenvalues' ratio is represented. Increasing either the maximum offset or the normalized RNMO beyond 1 in the *a priori* distribution, the number of degrees of freedom increases. The linear slope of N versus the maximum offset or RNMO p_{\max} is evident in Fig. 4a from the number of non-negligible eigenvalues of the covariance matrices corresponding to increasing RNMO spread (i.e. $dN/dx_{\max}^2 = dN/dp_{\max} \approx 1$). Obviously the number of detectable events, and their resolution, increases with the cable length. The number of degrees of freedom, N , is more or less independent of the *a priori* q distribution. This is shown in Fig. 4b where the eigenvalues of the covariance matrices are plotted versus increasing q distribution. This suggests that AVO information can be mistaken for the RNMO, if the $\{K\}$ subspace is wide enough to model the data.

Eigenvectors are an orthogonal basis of events that span the data space but they have no physical meaning. The contribution of each eigenvector of the basis could

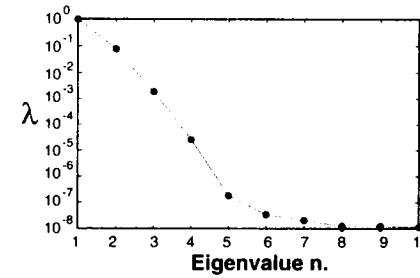


Figure 3. Eigenvalues of covariance matrix \mathbf{R} for uniform distribution of AVO and RNMO. Considering an eigenvalue spread of 30 dB which corresponds approximately to that signal-to-noise ratio, the number of degrees of freedom for this model is $N = 3$.

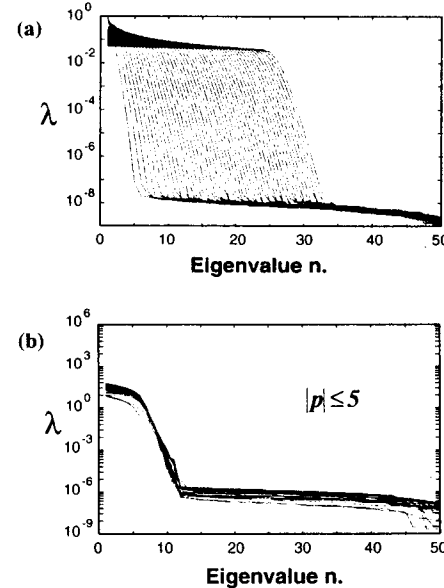


Figure 4. Eigenvalues of the covariance matrix \mathbf{R} : (a) for a uniform distribution of AVO and increasing RNMO (from $|p| < 1$ to $|p| < 25$) (or maximum offset; the normalized RNMO step is 0.5); (b) for a uniform distribution of RNMO ($|p| \leq 1$) and increasing AVO ($-1 \leq q \leq 1 + \delta q; \delta q = 0, 1, 2, \dots$). From the eigenvalue analysis it is evident that the number of degrees of freedom N increases almost linearly with the RNMO spread (a), but is almost independent of the AVO (b).

be evaluated using the residual

$$\|\varepsilon(p, q)\|^2 = \|\mathbf{a}(p, q) - \sum_{i=1}^N \beta_i \mathbf{v}_i\|^2, \quad (7)$$

with respect to the number N of eigenvectors considered and the parameters (p, q) . In this case, the first three eigenvectors span the data space with a residual below 1%, as predicted by the number of degrees of freedom.

Compound events decomposition of narrowband elastic reflections

Eigenvectors span the narrowband data subspace and, in general, are a useful tool for data filtering; however, an eigenvector cannot be used for seismic inversion due to its poor physical meaning. An alternative and more physical approach is the decomposition of the elastic reflections into a non-orthogonal basis of events: compound events decomposition (CED). Each compound event of the N th order corresponds to N interfaces properly spaced in time and RNMO $[\mathbf{a}_1, \mathbf{a}_2, \dots, \mathbf{a}_N]$, each vector of this basis \mathbf{a}_i depends only on p_i and q_i (i.e. $\mathbf{a}_i = \mathbf{a}(p_i, q_i)$). The narrowband data space could be spanned by a basis of events corresponding to compound events, each characterized by a pre-assigned RNMO and an AVO or by compound events with no AVO ($q_i = 0$), thus having RNMO only. In the Appendix A it is shown how to pre-assign optimally the RNMOs p_i of N th order CED given the covariance matrix of data space \mathbf{R} , resulting from the distribution of p and q . In Table 1 the values of RNMOs are given in the (AVO) column, the p_i for compound events with no AVO ($q_i = 0$) are given in the (NO-AVO) column.

The values of the mean-square error of the CED, with the RNMOs obtained for the uniform distribution of q and p , can be evaluated for decomposition into events with or without AVO (Appendix). Figure 5 shows the LMS error of CED with and without AVO versus increasing order N . Any reflection pertaining to the data set characterized by \mathbf{R} could also be described either by one event with AVO or by two events without AVO (see the spectrum ambiguity in Fig. 2), and either by two events with AVO or by four events without AVO. This demonstrates that any

Table 1. Normalized velocity sampling of non-orthogonal narrowband CED with and without AVO which minimizes the MS error for a population of reflections characterized by a uniform distribution of p, q .

N	p_i (NO-AVO)	p_i (AVO)
1	0	0
2	± 0.51	± 0.65
3	0; ± 0.76	0; ± 0.82
4	± 0.37 ; ± 0.89	± 0.34 ; ± 0.84

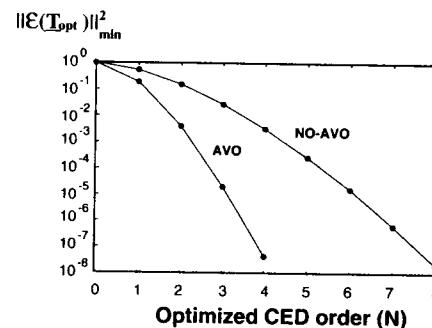


Figure 5. MS residual as a function of the number of reflections representing the data set. The *a priori* distribution that defines the data subspace can be described equivalently by a basis of N events with AVO (CED with AVO of N th order), or with $2N$ events without AVO (CED without AVO of $2N$ th order), obtaining a comparable residual.

elastic reflection, or any combination, can be decomposed into a compound event of the N th order with pre-assigned RNMO and AVO or of the $2N$ th order with pre-assigned RNMO but without AVO. Both descriptions obtained approximately the same LMS error but correspond to different media. The first-order compound event with AVO corresponds to the standard AVO analysis given the kinematic parameters (e.g. obtained from a velocity analysis), while the second-order compound event without AVO and pre-assigned RNMOs represents the combination of two events. This describes the data with a residual comparable to the AVO analysis.

Limited bandwidth extension of narrowband compound events decomposition

The analysis of narrowband data is a valuable guideline for moving towards a more physical CED of wideband CMP data. The optimal sampling of the p parameters, estimated for uniform distribution of RNMO of the reflections in the narrowband analysis, can be extended to limited bandwidth reflections. In this case analytical signals should be used, and small time delays correspond to phase shifts. As an example of limited bandwidth, let us consider reflections with centre frequency $f_0 = 30$ Hz and raised cosine bandwidth $\Delta f = 20$ Hz ($\Delta f < f_0$), a time window centred on $\tau = 0.5$ s, moveout velocity $v = 4000$ m/s (offset sampling $dx = 50$ m and the maximum offset $L = 2450$ m). Isolated CMP reflections with AVO and with a velocity error in the range of ± 90 m/s (this value corresponds to the normalized RNMO $p = \pm 1$) have been projected onto compound events given the normalized p sampling in Table 1. Figure 6a shows an example of the time windowed reflection with RNMO and AVO decomposed into N events without AVO, given the RNMO sampling of the basis. Increasing the number of events that

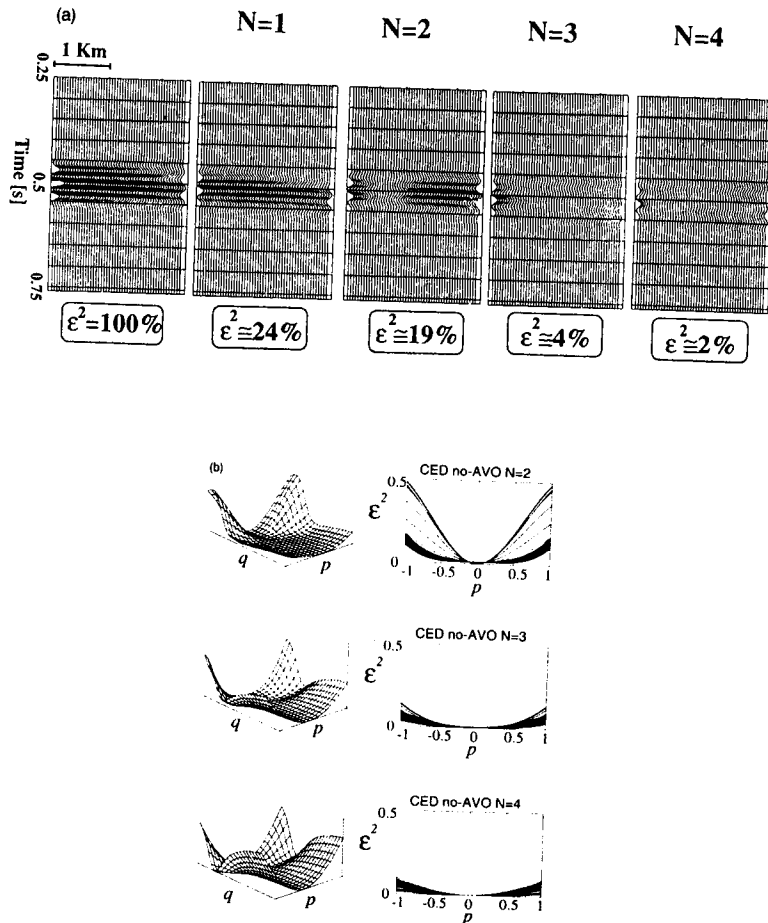


Figure 6. CED of limited bandwidth data ($f_0 = 30$ Hz, $\Delta f = 20$ Hz). (a): An example of the isolated reflection with AVO and velocity error is decomposed into compound events without AVO; the RNMO sampling is obtained from the narrowband analysis (Table 1: NO-AVO) vs increasing order $N = 1, 2, 3, 4$. (b) The residual depends on the original AVO and RNMO parameters q and p as well as on the CED dimensions; by increasing the CED order, the residual decreases as predicted for the narrowband model (Fig. 5) as the compound event spans the data space more accurately.

compose this basis results in a more accurate description of the reflections. The residual depends on N and the value (p, q) , associated with the reflection. Figure 6b shows the residual versus the reflection parameters for increasing N . The narrow-band equivalence (Fig. 5) between two events without AVO and one event with AVO can also be found in the limited bandwidth case. The case $N = 2$ without AVO and pre-assigned RNMO describes any reflection with AVO but without velocity error ($p = 0$ in Fig. 6b), with a residual below 5%.

Seismic data decomposition

Equivalent kinematic model of the compound events

The CED of wideband elastic reflections (i.e. using a full bandwidth wavelet $w(t)$) should contain the time dependence that was described by a simple phase shift in the limited bandwidth decomposition. If a reflection with normal incidence traveltime τ and moveout p is considered, the traveltimes of each event corresponding to the compound event to be used to describe that reflection are now

$$t_i(x) = \tau + \delta\tau_i + (p + \delta p_i)x^2. \quad (8)$$

The equivalent kinematic model corresponding to this compound event can be obtained from the moveout velocity v_i of the i th of the N composing events (8), i.e.

$$v_i^2 = \frac{v^2}{(1 + \delta\tau_i/\tau)(1 + \delta p_i/p)}. \quad (9)$$

Using the Dix formula approximation for the evaluation of the interval velocity V_i , it follows that

$$V_i^2 = -v^2 \frac{\delta p_i/p}{\delta\tau_i/\tau} \frac{1}{1 + \delta p_i/p} \approx -v^2 \frac{\delta p_i/p}{\delta\tau_i/\tau}. \quad (10)$$

To avoid non-physical velocities of the equivalent kinematic model (i.e. $V_i^2 < 0$), the condition

$$\delta p_i/\delta\tau_i < 0 \quad (11)$$

should hold (in (10) the RNMO is $|\delta p_i| \ll p$). The values of $\delta\tau_i$ as well as those of δp_i depend on the wavelet bandwidth as well as on the accuracy of the velocity analysis in the moveout evaluation. Figure 7 shows a schematic representation of the residual traveltimes of the events of the CED. The approach to the wideband CED is described below.

Compound events decomposition of wideband elastic reflections

In the wideband decomposition the residual traveltime of the i th event of the compound event is $\delta t_i(x) = \delta\tau_i + \delta p_i x^2$, from (8). The amplitude of the i th event of the compound event becomes $(A_i + B_i x^2)w(t - \delta t_i(x))$; each vector $\mathbf{a}_i(x)$ of the basis is

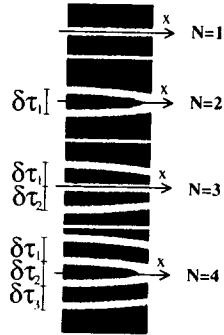


Figure 7. Schematic representation of residual traveltimes of wideband compound events after moveout correction. The traveltimes of the basis correspond to a 'fork', the relationship $\delta t_i(x) = \delta \tau_i + \delta p_i x^2$ holds for the i th prong. CED with $N = 1$ corresponds to velocity analysis (basis without AVO). For $N > 1$, a kinematically plausible model requires that $\delta p_i / \delta \tau_i < 0$ and this gives the shape to the prongs.

obtained by sampling at times t_1, \dots, t_m , thus

$$\mathbf{a}_i(x) = \mathbf{a}(x, \delta \tau_i, \delta p_i) = [w(t_1 - \delta t_i(x)), \dots, w(t_m - \delta t_i(x))]', \quad (12)$$

and corresponds to the wideband event at offset x (i.e. the space axis is continuous in the wideband basis). Let us consider a windowed and time-sampled signal $\mathbf{s}(x) = [s(x, t_1), \dots, s(x, t_m)]'$; if it is approximated by one compound event of order N , we get the residual

$$\begin{aligned} \iint \varepsilon^2(x, t) dt dx &= \int \left\| \mathbf{s}(x) - \sum_{i=1}^N (A_i + B_i x^2) \mathbf{a}_i(x) \right\|^2 dx \\ &= \int \left\| \mathbf{s}(x) - [\mathbf{T}(x, \delta \boldsymbol{\tau}, \delta \mathbf{p}), x^2 \mathbf{T}(x, \delta \boldsymbol{\tau}, \delta \mathbf{p})] \boldsymbol{\alpha} \right\|^2 dx, \end{aligned} \quad (13)$$

where

$$\mathbf{T}(x, \delta \boldsymbol{\tau}, \delta \mathbf{p}) = [\mathbf{a}_1(x), \mathbf{a}_2(x), \dots, \mathbf{a}_N(x)]. \quad (14)$$

The composite matrix $[\mathbf{T}(x, \delta \boldsymbol{\tau}, \delta \mathbf{p}), x^2 \mathbf{T}(x, \delta \boldsymbol{\tau}, \delta \mathbf{p})]$ corresponds to the CED with AVO while $\boldsymbol{\alpha} = [A_1, \dots, A_N, B_1, \dots, B_N]'$ is the vector of the amplitude coefficients (obviously, $B_1 = \dots = B_N = 0$ for CED without AVO). Figure 8 shows an example of the composite matrix for the case $N = 3$. In general, the residual between the signal and its projection onto the basis depends on the time and velocity sampling $\delta \boldsymbol{\tau} = [\delta \tau_1, \delta \tau_2, \dots, \delta \tau_N]'$ and $\delta \mathbf{p} = [\delta p_1, \delta p_2, \dots, \delta p_N]'$; the relationship (13), after some simplification, becomes

$$\|\varepsilon(\boldsymbol{\alpha}, \delta \boldsymbol{\tau}, \delta \mathbf{p})\|^2 = E_s + \boldsymbol{\alpha}' \Phi \boldsymbol{\alpha} - 2 \Psi (\delta \boldsymbol{\tau}, \delta \mathbf{p}) \boldsymbol{\alpha}, \quad (15)$$

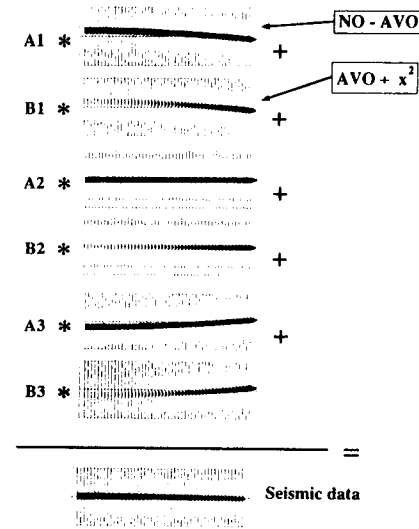


Figure 8. Example of wideband CED with $N = 3$. Each windowed reflection $s(x, t)$ characterized by a RNMO and an AVO is decomposed into a basis corresponding to a compound event characterized by AVO proportional to x^2 , pre-assigned lag $\delta \tau$ of the composing events and kinematically plausible RNMO as in (11). Here the RNMO has been exaggerated, for visual clarity, by a factor 4 with respect to its value normalized to half the main lobe of the wavelet over the effective aperture L .

where $E_s = \int \mathbf{s}(x)' \mathbf{s}(x) dx$ is the signal energy. The symmetric positive-definite matrix $\Phi = \int [\mathbf{T}(x), x^2 \mathbf{T}(x)]' [\mathbf{T}(x), x^2 \mathbf{T}(x)] dx$ is the basis correlation matrix; each element is the autocorrelation of the wavelet evaluated at offset-dependent time delay. The residual (15) depends also on the cross-correlation between the basis and the data $\Psi = \int \mathbf{s}(x)' [\mathbf{T}(x), x^2 \mathbf{T}(x)] dx$. From (15) it follows that the residual is quadratic in the AVO parameters, while non-linear in the time and velocity sampling. Optimizing with respect to the AVO parameter vector $\boldsymbol{\alpha}$, the LMS error becomes

$$\|\varepsilon(\delta \boldsymbol{\tau}, \delta \mathbf{p})\|_{\min}^2 = E_s - \Psi \Phi^{-1} \Psi', \quad (16)$$

which is the wideband equivalent of the narrowband CED (see relation (A3) in the Appendix). The optimal time sampling of the basis should be evaluated for each distribution of the signal parameters (i.e. AVO behaviour and velocity errors) under the kinematical constraint (11). The time intervals between the elementary events depend on the wavelet bandwidth. For a Ricker wavelet, the fixed time interval $\delta \tau_i = \delta \tau \approx 1/f_r \sqrt{2\pi}$ is a reasonable choice as this is the time resolution for the Ricker bandwidth. For the RNMO sampling, the values of Table 1 derived in

the Appendix can be adopted, provided that the normalized narrowband RNMO value $p = 1$ now corresponds to $\delta p \approx 1/L^2 f_r \sqrt{2\pi}$. Time intervals as well as RNMOs of wideband CED are pre-assigned and normalized to half the main lobe of the wavelet.

Given the data $\xi(x, t)$, the search for the combination of the kinematic and amplitude parameters minimizing the overall residual within a time window corresponds to a non-linear optimization of (16). Given an approximate velocity estimation v , this velocity analysis with AVO is an alternative approach to a joint search for AVO and velocity parameters. In other words, the projections onto $\{A\}$ and $\{K\}$ would be optimized in order to minimize the overall residual. The quality and the reliability of the velocity analysis with AVO is considerably better than spatial coherence measurements of classical velocity analysis (e.g. semblance); however, a detailed description is beyond the scope of this paper.

Derivation of the equivalent kinematic model: an example

As an example of the application of CED, a synthetic CMP obtained using reflectivity modelling has been analysed. The processing sequence adopted for the CMP data is (using a Ricker wavelet of $f_r = 60$ Hz):

- (1) geometric spreading correction;
- (2) muting of refracted arrivals;
- (3) velocity analysis and picking;
- (4) static NMO correction for each picked reflection.

Figure 9 shows the CMP gather for the elastic model and the velocity spectrum of

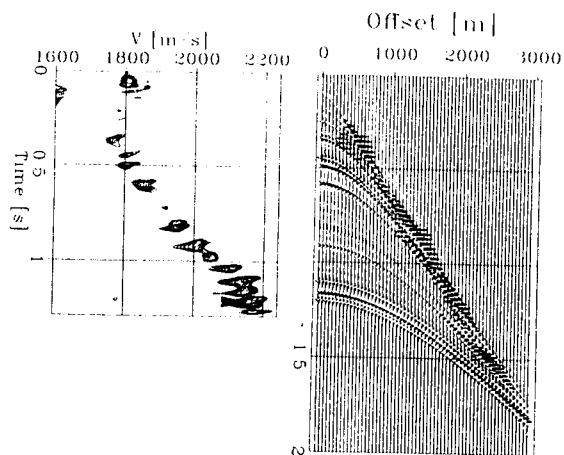


Figure 9. Seismic data decomposition. CMP seismogram of a synthetic elastic model using a Ricker wavelet with $f_r = 60$ Hz and its velocity analysis (21 interfaces).

the muted data using standard coherence measurements. The data model has been obtained from a well-log profile where the number of interfaces have been identified as 21. The kinematic parameters (τ_i, v_i) , $i = 1, \dots, M$ for $M = 13$ complex reflections, are easily detected from the coherence peak of the velocity spectrum. Each windowed reflection, after NMO correction for the estimated moveout parameters, has been projected onto bases of N events with AVO, as in (13). The time sampling of the compound events is fixed and dependent on the wavelet bandwidth ($\delta\tau = 1/f_r \sqrt{2\pi} \approx 6.5$ ms). Also the RNMO sampling is fixed for each event of the CED and every order N : $\delta p \approx -0.5\delta\tau/L^2$ where L is the effective aperture after muting (for the sake of simplicity δp has been assumed to be independent of the CED order and approximately equal to narrowband NO-AVO CED with $N = 2$, as in Table 1). Equations (1) and (9) give the corresponding moveout error for each reflection of the compound event. In this example the RNMO of the compound events is below 10 m/s. By increasing the dimensions N of the CED used to describe the data the residual computed on the overall CMP data is reduced as shown in Fig. 10. Owing to velocity errors and interference of the 21 interfaces of the original model, we represent data with $M = 13$ compound events. Classical AVO (i.e. CED with $N = 1$) is inaccurate since in this example it corresponds to the measurement of AVO of interfering reflections with velocity errors.

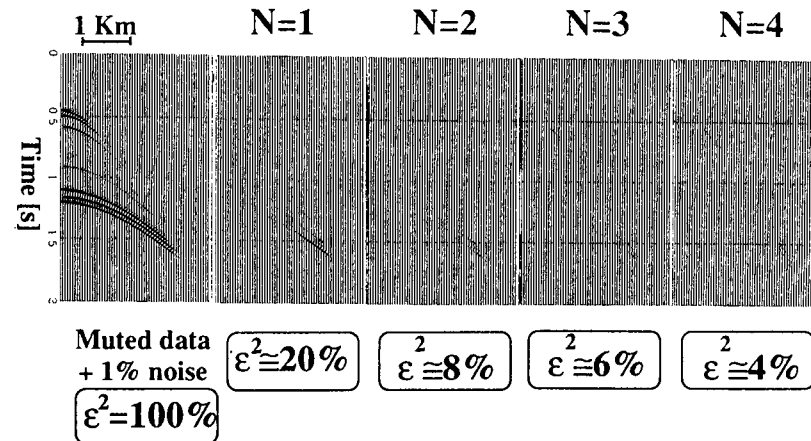


Figure 10. Residuals of the CED of $M = 13$ reflections detected from the velocity spectrum of muted CMP data (Fig. 9) vs increasing order N of the CED. The time lags $\delta\tau$ and RNMO δp within each compound event are predetermined: $\delta\tau \approx 6.5$ ms and $\delta p \approx 3.3$ ms/ L^2 . These values correspond to a velocity error of the compound events that is below 10 m/s. 1% of noise has been added as a visual reference for the residual evaluation.

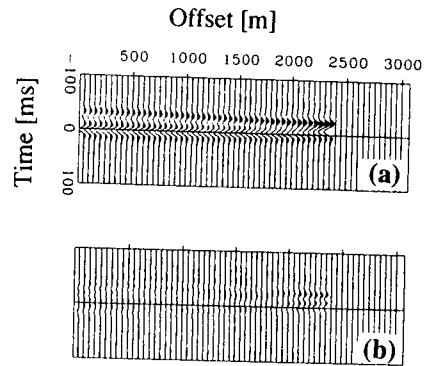


Figure 11. Detail of the decomposition shown in Fig. 10. (a) The reflection indicated by an arrow in Fig. 9 at the moveout parameters $\tau_{12} = 1200$ ms and $v_{12} = 2160$ m/s, and (b) the residual (approximately 2%) after the CED with $N = 3$.

The optimized RNMO of the compound event with $N = 1$ and uniform velocity uncertainty is $\delta p = 0$ and this is in agreement with the common practice of measuring the AVO along the traveltime obtained from a coherence peak. Increasing the order to the CED, the residuals reduce as expected. However, even if the macro-model remains approximately unchanged, the detailed description of the interfaces depends on the number of events of the CED. The behaviour of the residual versus the compound event order shows that $N = 3$ is a good compromise (Fig. 11).

The equivalent kinematic model using the compound AVO basis with $N = 3$ (Fig. 12) is able to describe the muted CMP within a residual of 2–4% while the RNMO δp is approximately 0.4% of the moveout of the data.

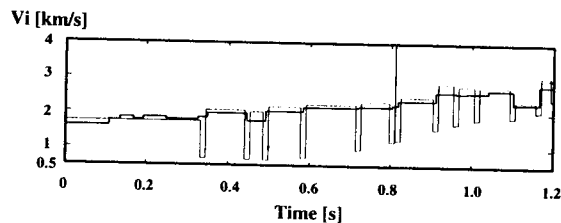


Figure 12. The kinematically equivalent model (CED with $N = 3$, thin line) and the elastic model (thick line) for the synthetic CMP in Fig. 9. Even if the equivalent kinematic model were geologically meaningless, the inversion is unable to differentiate between the solutions in the kinematic subspace without any *a priori* information.

The N th order CED describes the CMP data using, for each complex reflection identified as a coherence peak, N events with AVO and a fixed relative time location of the interfaces. As each compound event is defined by its global moveout parameters τ and v , and each compound event is described by its AVO parameters (A_i, B_i) , the overall parameters for M detected reflections are $M \times 2 + M \times (2N)$: hence, the CED corresponds, in general, to data compression. The example shown here, and personal experience suggest that applying a CED with $N = 2$ or 3 and fixed lags that depend on the data bandwidth, is accurate enough for the common signal-to-noise ratio of seismic data. This dimension of the compound event is also in agreement with the number of degrees of freedom of narrowband data shown in Fig. 3.

Discussion and conclusions

The unreliability of the MS solution of AVO analysis and inversion was explored. It was found that interfering seismic reflections with velocity errors can be replaced by compound events without AVO, and this makes the reliability of AVO inversion questionable. Furthermore it was shown that the presence of AVO does not generally increase the number of degrees of freedom of the data. It was demonstrated that any combination of narrowband elastic reflections with velocity errors can be decomposed into either an N th order compound event with AVO or a $2N$ th order compound event without AVO, the residuals being comparable. For instance, standard AVO analysis coincides with the $N = 1$ CED with AVO. $N = 2$ CED without AVO achieves the same residuals. The number of events that span the same data space is fixed when considering either an orthogonal basis (eigenvectors) or a non-orthogonal basis (CED). Moreover, the statistical analysis has shown the equivalence between the bases.

The CED with and without AVO has been extrapolated to the bandwidth of practical seismic data. The Ricker wavelet CED was also examined in a synthetic example using a physically possible velocity sampling. A geophysically, but not geologically, plausible medium is determined that is equivalent to the original elastic model.

Acknowledgements

The author is grateful to Fabio Rocca for his encouragement, guidance and many suggestions, all of which were indispensable to the development and completion of this work.

The work was partially funded by AGIP SpA (Italy) within the framework of the Geoscience Project sponsored by the CEC, DG XII, Contract JOUF 0037.

Appendix A

Narrowband CED

Let us consider the basis with both RNMO and AVO: each vector of this basis \mathbf{a}_i depends only on p_i and q_i (i.e. $\mathbf{a}_i = \mathbf{a}(p_i, q_i)$); thus, any narrowband situation can be decomposed into the linear combination of N events that together form the matrix \mathbf{T} , given by

$$\mathbf{T} = [\mathbf{a}_1, \mathbf{a}_2, \dots, \mathbf{a}_N]. \quad (\text{A1})$$

Any narrowband elastic reflection $\mathbf{a}(p, q)$ modelled from (4) will now be approximated by the product of the matrix \mathbf{T} times a vector $\boldsymbol{\alpha}(p, q)$ that depends on the reflection parameters (p, q) , thus

$$\mathbf{a}(p, q) \simeq \mathbf{T}\boldsymbol{\alpha}(p, q). \quad (\text{A2})$$

Minimizing the error, we find the value of $\boldsymbol{\alpha}(p, q)$; the LMS error then becomes

$$\|\boldsymbol{\epsilon}(p, q, \mathbf{T})\|_{\min}^2 = \mathbf{a}^*(p, q)(\mathbf{I} - \mathbf{P})\mathbf{a}(p, q). \quad (\text{A3})$$

The matrix $\mathbf{P} = \mathbf{T}(\mathbf{T}^*\mathbf{T})^{-1}\mathbf{T}^*$ corresponds to the projection of $\mathbf{a}(p, q)$ onto the subspace spanned by the non-orthogonal basis \mathbf{T} . The MS error for an optimal choice is better expressed as

$$\|\boldsymbol{\epsilon}(p, q, \mathbf{T})\|_{\min}^2 = \text{Tr} \{(\mathbf{I} - \mathbf{P})\mathbf{a}(p, q)\mathbf{a}^*(p, q)(\mathbf{I} - \mathbf{P})\}. \quad (\text{A4})$$

For each (p, q) , the MS error (A4) depends only on the chosen basis \mathbf{T} . For any *a priori* statistical distribution, the MS error becomes

$$E[\|\boldsymbol{\epsilon}(\mathbf{T})\|^2] = \text{Tr} \{(\mathbf{I} - \mathbf{P})E[\mathbf{a}(p, q)\mathbf{a}^*(p, q)](\mathbf{I} - \mathbf{P})\} = \text{Tr} \{(\mathbf{I} - \mathbf{P})\mathbf{R}(\mathbf{I} - \mathbf{P})\}. \quad (\text{A5})$$

The residual depends on the covariance matrix \mathbf{R} for the given distribution once \mathbf{T} has been chosen. We use the probability density of p and q to define the covariance matrix; then, we find the optimal \mathbf{T} that minimizes the MS residual (A5), given the covariance matrix. From (A5), the minimization is obtained from the gradient computation

$$\frac{\partial E[\|\boldsymbol{\epsilon}(\mathbf{T})\|^2]}{\partial(p_1, p_2, \dots, p_N)} = 0. \quad (\text{A6})$$

A signal-to-noise energy ratio of 10^3 is considered in the computation of the projection matrix \mathbf{P} to optimize the p_i , $i = 1, \dots, N$, as this value can be compared to 'good quality' seismic data. For this purpose, from the SVD of the basis \mathbf{T} : $\mathbf{U}^*\mathbf{T}\mathbf{V} = \boldsymbol{\Lambda} = \text{diag}(\lambda_1, \lambda_2, \dots, \lambda_N)$, the singular value spread of 10^3 defines the matrix of the singular values $\boldsymbol{\Lambda}_S$ and the factorization of \mathbf{T} becomes (Golub and Van Loan 1989)

$$\mathbf{T} \simeq \mathbf{U}_S \boldsymbol{\Lambda}_S \mathbf{V}_S^* = \sum_{i=1}^S \lambda_i \mathbf{u}_i \mathbf{v}_i^*, \quad 1 > \frac{\lambda_2}{\lambda_1} > \dots > \frac{\lambda_S}{\lambda_1} \geq 10^{-3} > \dots > \frac{\lambda_N}{\lambda_1}; \quad (\text{A7})$$

the projection matrix for the evaluation of (A6) is $\mathbf{P} = \mathbf{U}_S \mathbf{U}_S^*$. The optimization procedure of (A6) yields the optimized RNMOs' p_i for any given distribution of p and q . Table 1 gives the p_i values for a uniform distribution of p and q .

References

- de Haas J.C. and Berkhout A.J. 1990. On the information content of P-P, P-SV, SV-SV and SV-P reflections. 60th SEG meeting, San Francisco, Expanded Abstracts, 1190-1194.
- Folstad G. and Schoenberg M. 1992. Use of equivalent anisotropic medium theory to calculate synthetic AVO response. SEG/EAGE workshop, Big Sky, Montana, USA, August 1992, Expanded Abstracts, 614-621.
- Golub G.H. and Van Loan C.F. 1989. *Matrix Computations*. Johns Hopkins Press, Baltimore, MD.
- Herbert W.S. 1991. Amplitude-versus-Offset measurement errors in a finely layered medium. *Geophysics* 56, 41-49.
- Kolb P., Collino F. and Lailly P. 1986. Pre-stack inversion of a 1-D medium. *Proceedings of the IEEE* 74, 498-508.
- Shuey R.T. 1985. A simplification of the Zoeppritz equations. *Geophysics* 50, 609-614.
- Spratt S. 1987. Effect of Normal Moveout errors on amplitude versus offset-derived shear reflectivity. 57th SEG meeting, New Orleans, Expanded Abstracts, 634-637.
- Tarantola A. 1986. A strategy for nonlinear elastic inversion of seismic reflection data. *Geophysics* 51, 1893-1903.
- Tarantola A. 1987. *Inverse Problem Theory*. Elsevier Science Publishing Co., Amsterdam.
- Van Rijssen E.P.F. and Herman G.C. 1991. Resolution analysis of band-limited and offset-limited seismic data for plane-layered subsurface models. *Geophysical Prospecting* 39, 61-76.
- Walden A.T. 1991. Making AVO sections more robust. *Geophysical Prospecting* 39, 915-942.